Present and Past-Millennial Eutrophication in the Gulf of Gdańsk (Southern Baltic Sea)

M. Szymczak-Żyła[1] [ID], **M. Krajewska[1]**, **M. Witak[2]** [ID], **T. M. Ciesielski[3]**, **M. V. Ardelan[4]**, **B. M. Jenssen[3,5]** [ID], **T. Goslar[6,7]**, **A. Winogradow[8]**, **A. Filipkowska[1]**, **L. Lubecki[1]**, **A. Zamojska[9]**, and **G. Kowalewska[1]** [ID]

[1]Marine Pollution Laboratory, Institute of Oceanology, Polish Academy of Sciences, Sopot, Poland, [2]Faculty of Oceanography and Geography, Institute of Oceanography, University of Gdańsk, Gdynia, Poland, [3]Department of Biology, Norwegian University of Science and Technology, Trondheim, Norway, [4]Department of Chemistry, Norwegian University of Science and Technology, Trondheim, Norway, [5]Department of Bioscience, Aarhus University, Roskilde, Denmark, [6]Faculty of Physics, Adam Mickiewicz University, Poznań, Poland, [7]Poznań Radiocarbon Laboratory, Poznań Park of Science and Technology, Poznań, Poland, [8]Department of Marine Chemistry and Biochemistry, Institute of Oceanology, Polish Academy of Sciences, Sopot, Poland, [9]Department of Econometrics, Faculty of Management, University of Gdańsk, Sopot, Poland

Abstract Eutrophication is manifested by increased primary production leading to oxygen depletion in near-bottom water and toxic cyanobacteria blooms. This is an important contemporary problem of the Baltic Sea and many other coastal waters. The present eutrophication is mainly ascribed to anthropogenic activity. To compare the present trophic state with that during past millennia, two sediment cores (50 cm long and ~400 cm long covering ca. 5,500 years) were taken from the Gulf of Gdańsk (southern Baltic Sea). The core subsamples were analyzed for phytoplankton pigments (chlorophylls and their derivatives, and carotenoids). In addition, carbon (C_{tot}, C_{org}, and $\delta^{13}C$), ^{14}C dating, grain size, diatoms, and selected metals in the cores were analyzed to determine conditions in the depositional environment. The results indicated that there were high primary production periods in the past, during the Littorina Sea and the Roman Climatic Optimum, accompanied by oxygen deficiency in the near-bottom water, most probably caused by climate warming. The ratio of $13^2,17^3$-cyclopheophorbide-a enol, a labile degradation product of chlorophyll-a, to the sum of other chloropigments-a (CPPB-aE/ΣChlns-a) is proposed as a new paleoredox proxy. Heterocystous cyanobacteria blooms of an intensity similar to or even greater than at present also occurred in past millennia and were connected with climate warming. Hence, eutrophication must have occurred in the past, which means that natural factors have a substantial influence on it.

1. Introduction

In the last century eutrophication has become a worldwide problem in enclosed aquatic basins, semi-enclosed seas, and coastal zones (Conley et al., 2011; EC, 2000, 2008; Orive et al., 2002; Xue et al., 2007). There are different definitions of the term *eutrophication*. Some explain it as a process, some as a state of the environment, and others describe it as the input of nutrients into the environment. According to Helsinki Commission (HELCOM, 2009) *eutrophication* means "well nourishing" (in fact "overnourishing") and its adverse consequences for the environment. The most frequently mentioned causes of present eutrophication are excess nutrient input and the change of the limiting nutrient, both mainly anthropogenic. However, natural input of organic matter and hydrometeorological conditions may also be important (Ambio, 1990). "Overnourishing" results in greatly increased primary production, and this may also lead to toxic cyanobacteria blooms. Additionally, when there is no water mixing, turbidity increases as a result of phytoplankton and macrophyte senescence and death with the subsequent settlement of decay products on the seabed, where they undergo diagenesis. A high sedimentation rate, together with a lack of wave action and water currents, leads to oxygen deficiency in the near-bottom water (Conley et al., 2009).

In the Baltic Sea tides are negligible and water exchange with the North Sea is restricted. Moreover, the Baltic receives freshwater from a catchment area inhabited by approximately 80 million people. Therefore, this water body is sensitive to anthropogenic nutrient pollution (Conley et al., 2009; HELCOM, 2007, 2014). The Gulf of Gdańsk (southern Baltic, Poland) is especially affected by eutrophication as a result

of its topography and location (HELCOM, 2013) and large water inflow from the Vistula River (Wisła). The Vistula River is the second largest river draining into the Baltic and discharges water from nearly half of Poland (Majewski, 1990). This primarily influences the salinity and causes the deeper waters of the Gulf of Gdańsk to stratify because of the difference in density between the Vistula freshwater and Baltic seawater. A halocline prevents the vertical mixing of the water masses, leading to oxygen deficiency in the near-bottom water. This near-bottom water is exchanged only after strong inflows of saline, oxygenated water from the North Sea through the Danish Straits, usually during winter storms occurring once every 5 to 10 years (Matthäus et al., 2008). In addition, over the last millennium, the Gulf of Gdańsk has been subject to anthropogenic impacts resulting from urbanization, industrialization, and port and shipyard activities, all of which have intensified during the last 100 years. This has exacerbated the eutrophication of the Gulf, adding to the impact of the nutrient load transported there by the Vistula from Poland.

Determination of the phytoplankton pigment concentrations, that is, chloropigments and carotenoids, in recent sediments is a good method of tracking trends in eutrophication (Krajewska et al., 2019; Szymczak-Żyła et al., 2017). The pigment concentration in sediments depends on a number of factors associated with primary production, sedimentation/accumulation, and postdepositional conditions in sediments, and also on pigment stability. The recent eutrophication of the Gulf of Gdańsk is reflected in the high chloropigment-a content in surface Gdańsk Deep sediments, especially where laminated sediments have been deposited (Szymczak-Żyła et al., 2017). Further, a study on sediments from the Gulf of Gdańsk deposited during recent millennia (Szymczak-Żyła & Kowalewska, 2009) revealed that chloropigments-a were present along the entire core length in fluctuating concentrations. In that study, the chloropigment-a profile suggested that primary production may have been even greater ca. 2,000 years ago than in present-day conditions. That work corroborated previous studies on chloropigments in old (up to 8,000 years) sediments from the eastern Gotland Basin and other deep basins in the Baltic (Kowalewska, 2001; Kowalewska et al., 1998, 1999). In addition, the evidence of past cyanobacteria blooms has been suggested by Bianchi et al. (2000), who found considerable amounts of the carotenoid zeaxanthin present in deep sediments from the north western Baltic formed 7,500 years BP. Pountanen and Nikkilä (2001), who studied cyanobacteria carotenoids in sediment cores from the Gotland Basin, the open northern Baltic Proper, and the eastern Gulf of Finland, came to the same conclusions. These and other reports of present-day blooms of diazotrophic cyanobacteria elsewhere in the world (Carpenter et al., 1993; Cook et al., 2016; Paerl, 1988) suggest that eutrophication caused by natural factors can be considerable.

The aim of this work was to address the importance of natural factors in the occurrence of eutrophication. Thus, we investigated temporal variations in levels of primary production, oxygen conditions, and toxic cyanobacteria abundance during the last millennia in the Gulf of Gdańsk. This objective was achieved by a multiproxy analysis of core sediments and statistical investigation of the analytical results. The sediment samples were analyzed for phytoplankton pigments (chlorophylls and their derivatives, including $13^2,17^3$-cyclopheophorbide-a enol [CPPB-aE], and carotenoids), diatoms, selected metals, carbon (C_{tot}, C_{org}, $\delta^{13}C$), ^{14}C dating, and grain size, and next various proxies were used for reconstruction of changes in primary production level, oxygen conditions, and phytoplankton composition in the Gulf of Gdańsk during the past millennia.

2. Materials and Methods

2.1. Sediment Sampling

A long sediment core (384 cm) was collected using a vibrocorer (VKG-6/3) during the research cruise of R/V IMOR (Maritime Institute in Gdańsk, Poland) in April 2015 at station P116 in the Gdańsk Deep (54°39.040′ N, 19°17.240′E; water depth: 89 m; Figure S1 in the supporting information). Before the sediment core was taken, the seabed was scanned (200 × 200 m) with a multibeam echosounder in order to locate potentially undisturbed sampling sites. After collection, the core was cut into 100-cm-long sections and transported to the laboratory where the sections were subdivided into 2-cm-thick layers. These subsamples were transferred to polyethylene bags/containers and stored in a deep freeze (−20 °C) until analysis. Sediment handling was performed under nitrogen-protective atmosphere. To estimate the length of the topmost section of the long core, which was lost during vibrocorer collection, an additional short core (50 cm) was taken with a GEMAX core sampler, at the same location. This latter core was also divided into 2-cm-thick layers.

2.2. ^{14}C Dating

Eleven selected sediment samples (bulk organic matter) from the long core layers and one shell were radiocarbon dated at the Poznań Radiocarbon Laboratory using accelerator mass spectrometry (Goslar et al., 2004). As in a previous extensive study of the whole Baltic (Kabel et al., 2012), ^{14}C analysis of sediment samples was performed on the NaOH soluble (humic acids [HA]) and the base residue (humins [RES]) fractions (Brock et al., 2010; Kigoshi et al., 1980). The results were calibrated using Marine13 curve (Reimer et al., 2013). The local correction for the reservoir age Delta-$R = -50 \pm 100$ years was calculated on the basis of the 14CHRONO Marine Reservoir Database.

2.3. Grain-Size Analysis

Sediment samples were analyzed by laser diffraction (Fritsch Laser Particle Sizer Analysette-22; Kramarska et al., 1996) and recorded with a resolution of 1ϕ. Sodium pyrophosphate was used to prevent aggregates forming during measurement. To remove organic matter, all sediment samples were treated with 30% H_2O_2 prior to analysis.

2.4. Diatom Analysis

Samples for qualitative diatom analysis were prepared following the standard method described by Battarbee (1986). For quantitative analyses, a random settling technique was used (Bodén, 1991) and the concentration of diatoms per unit weight of dry sediment was estimated. Permanent diatom preparations were mounted in Naphrax® (refractive index $n_D = 1.73$). The analysis was performed with a Nikon microscope under a 100X oil immersion objective. From 500 to 800 valves were counted in each sample to estimate the percentage abundance of the various taxa (Schrader & Gersonde, 1978). Raw counts were converted into relative abundance of the total frustules counted. The taxonomy was based primarily on Krammer and Lange-Bertalot (1986, 1988, 1991a, 1991b), Hasle and Syvertsen (1996), and Håkansson (2002). The diatoms were divided into groups according to their biotope, salinity, and temperature requirements using OMNIDIA 5.3 software (database 2012). Based on species composition and the relative frequency of planktic taxa, diatom assemblage zones were distinguished using cluster analysis in TILIA 2.0.37.

2.5. Carbon Analysis

Total (C_{tot}) and organic (C_{org}) carbon as well as the stable carbon ($\delta^{13}C$) isotope were analyzed in a Flash EA 1112 Series Elemental Analyzer combined with a Delta V Advantage Isotopic Ratio Mass Spectrometer (Thermo Electron Corp., Germany). For C_{org} analyses, dry, homogeneous samples of the sediments were weighed into silver vials and acidified with 2-M HCl (Chang et al., 1991; Hedges & Stern, 1984). The C_{org} concentration was expressed as the percentage of the bulk of the dry sample after removal of carbonates. Quality control of the organic carbon measurements was carried out with standards (Thermo Electron Corp.). The accuracy and precision (average recovery 99.1% $\pm$ 2.0%) of the methodology were deemed to be satisfactory. Inorganic carbon (C_{inorg}) was determined as the difference between total and organic carbon. Isotopic ratios $\delta^{13}C$ were calculated using the laboratory working pure reference gas CO_2 calibrated against International Atomic Energy Agency standards: CO-8 and USGS40. The $\delta^{13}C$ results are given in the conventional delta notation, that is, versus Pee Dee belemnite.

2.6. Pigment Analysis

The pigment extraction, analysis, and quantification were carried out using the procedures described in detail elsewhere (Krajewska et al., 2017; Szymczak-Żyła, 2018; Szymczak-Żyła et al., 2008, 2017). In brief, ultrasound-assisted extraction of wet sediment samples with acetone was applied. Next, liquid-liquid extraction was performed in the acetone extract:benzene:water system. The benzene layer was evaporated to dryness in a stream of argon and stored frozen (-20 °C) until high-performance liquid chromatography (HPLC) analysis. Pigments were separated using an HPLC system (HPLC set; Knauer, Germany) equipped with two detectors: diode array (DAD 2800 Knauer) and fluorescence detector (RF-20Axs, Shimadzu, Japan). The pigments were separated on a Lichrosapher 100RP-18e column (250 × 4 mm, 5 μm; Merck, Germany). Pigments were identified on the basis of retention time and absorbance spectra compared with pigment standards (DHI Lab Products, Denmark).

2.7. Metal Analysis

The total concentrations of each of the metals in the sediment samples were calculated as the sum of their respective concentrations in four fractions. The metals were extracted using a modified European Community Bureau of Reference (BCR) three-step sequential procedure (Ardelan et al., 2009; Usero et al., 1998) followed by digestion with nitric acid in a high-pressure microwave system (Milestone UltraClave, EMLS, Leutkirch, Germany; sequential extraction was applied because of the requirements of another, related study on the same sediment cores). Final concentrations of the metals in the extracts were determined by inductively coupled plasma high-resolution mass spectrometry using a Thermo Finnigan model Element 2 instrument (Bremen, Germany) with an SC-FAST flow injection analysis system (Elemental Scientific, Inc., Omaha, USA). Analysis of sediment lake certified reference materials BCR-701 showed good agreement between the results and the certified values.

2.8. Statistical Analysis

The results were statistically processed using STATISTICA 9.0 and EViews 9.0 software. Initially, the time properties of the long core data series were tested. The augmented Dickey-Fuller test was used to identify the integration order of the series. Thereafter, the autocorrelation function and the partial autocorrelation function were applied to quantify how a variable series was correlated with itself at different lags (Dickey & Fuller, 1979; Fuller, 2009). Then the Hodrick-Prescott filter (for separating cyclic behavior from the long-run path of the time series) was used to divide changes in the time series of the primary production, oxygen deficiency, and phytoplankton composition proxies into trend and cycle components and then to calculate cross-proxy correlations for the fluctuations in both of these components. Using cluster analysis, a classification of the long core layers, taking into account the oxygen deficiency proxy values, was created.

3. Results

3.1. Age Model

Calibrated ^{14}C ages versus depth are presented in Figure 1 and in Table S1 in the supporting information. It has been assumed, based on chloropigment-a results, that the uppermost 20-cm section of the long core was lost during collection (see section 3.5). [14]C ages of the RES fraction of sediments appear systematically older than those of the HA fraction. Two-fraction ^{14}C analysis has been applied mostly to soil dating (e.g., Kristiansen et al., 2003; Mayer et al., 2008; Tonneijck et al., 2006). Most such studies show that the HA illuviated from upper organic horizons appears younger than the RES, which may bear carbon from reworked organic material. Hence, HA ages are regarded as minimum ones for the onset of pedogenesis, whereas RES ages are interpreted as maximum ages for burial. In this context, concordant ^{14}C ages of the two fractions at a certain soil level signify that they truly represent the formation time of this level. In this sense, the concordant ages of the two fractions of Baltic sediments, studied by Kabel et al. (2012), indicate that these ages are representative of the time of deposition at the spot cored. In our study (Figure 1), the ^{14}C ages of the two (HA and RES) fractions cluster along two separate lines, with the HA line roughly fitting the calibrated age of the shell (at 368–370 cm), whereas the RES line is distinctly older. Therefore, we believe that HA ages roughly represent the time of sedimentation on the sea floor, whereas RES ages are older because of the major contribution of reworked material in this fraction.

Whichever line indicates the sedimentation time, it is obvious that at each depth, the sediment is a mixture of material of different ages, containing organic carbon of different ^{14}C signatures. Since all the analytical work presented in this paper was performed on bulk material, except for ^{14}C analysis, we suggest using a working age-depth model (the most suitable for presenting and discussing the results of other analytical work) as the average of those for the HA (plus the shell) and RES fractions. This working age-depth model indicates that the long sediment core collected from the Gdańsk Deep covers ca. 5,500 calendar years (Figure 1). Over most of the profile, the uncertainty of the working model, related to the difference between the HA and RES models, is close to ±300 years, except for the uppermost and lowermost sections of the profile.
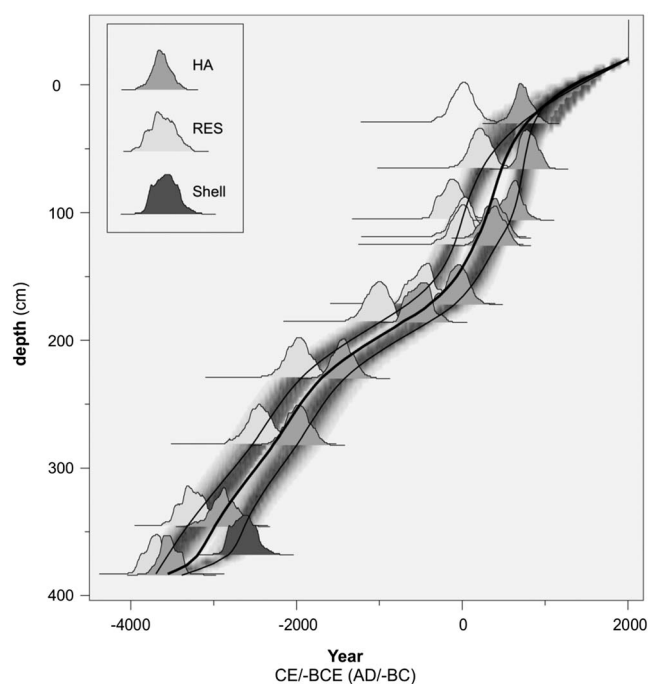
Figure 1. Age-depth model of the long core analyzed in this work. The two models for the humic acid (HA; plus the shell) and the humin (RES) fractions were calculated using the free-shape algorithm published by Goslar et al. (2009). Silhouettes (with types of dated material distinguished by gray fillings) represent probability distributions of calibrated ^{14}C dates of individual samples, while the gray bands represent the uncertainties of the two models. The age of one RES fraction (at 28–30 cm) was rejected from the model calculations. The working model—the average of those for HA and RES—is depicted by the thick line.

3.2. Grain Size

According to Shepard's (1954) classification, all the analyzed samples consisted of clayey silt sediments. In the samples analyzed from this core, the fine-grain-size fraction (<0.004 mm) content was from 28% to 44%. Only one of these samples contained a small (~0.1%) sand fraction >0.063 mm (308–310 cm).

3.3. Diatoms

A total of 191 diatom species, subspecies, varieties, and forms were identified in the whole material. Planktic diatom flora predominated in all the samples (Figure 2). Amongst these, euhalobous (marine) taxa occurred abundantly with cold-water species (*Coscinodiscus marginatus*, *C. oculus-iridis*, *Rhizosolenia hebetata* f. *hebetata*, and *Pauliella taeniata*), warm-water species (*C. radiatus*, *Pseudosolenia calcar-avis*, *Thalassionema nitzschioides*, *Thalassiosira eccentrica*, and *T. levanderi*), and cosmopolitan species (*Actinocyclus octonarius*, *C. asteromphalus*, *C. centralis*, *C. granii*, *C. obscurus*, and *T. anguste-lineata*). These species were accompanied by mesohalobous (brackish-water) taxa, and cold-water (*T. baltica*) and cosmopolitan taxa (*Cyclotella choctawhatcheeana* and *T. lacustris*) were most often observed in this group. The temperature preferences of *Chaetoceros* spp. RS are unknown. Rarely noted were oligohalobous, halophilous, and indifferent (freshwater) planktic species making up the allochthonous (i.e., riverine) component of the diatom flora. Based on the floristic spectrum, the relative abundance of dominant and subdominant taxa, and the relations between the percentage content of the ecological groups, five diatom assemblage zones were distinguished in the core (Figure 2 and Table S2 in the supporting information).

The percentage of warm-water diatoms (WWD) was used in this paper as a water temperature proxy. The relative abundance of WWD (Figure 3a) was depth variable and ranged from ~3% to ~55%. Higher values were found in two sections of the sediment core—from ~70 to ~200 cm and from ~310 to ~384 cm. In the short core (Figure 4a), percentages were higher (up to 50%) in the top 16-cm section of the core.

3.4. Carbon

Organic carbon (C_{org}) concentrations ranged between 2.6% and 7.4% in the long sediment core (Figure 3b). Highest concentrations were found in two sections of the sediment core—from ~80 to ~220 cm and from ~300 to ~384 cm. Analysis of total carbon (C_{tot}) in the selected sediment samples showed the inorganic carbon content (C_{inorg}) to be low—between 0.3% and 1.3%.

The "traditional" proxy profile used for determining organic matter sources, $\delta^{13}C$, is shown in Figure 3c. The $\delta^{13}C$ values (between −24.6‰ and −25.9‰) measured in the sediment core indicate that organic matter was a mixture of terrestrial and marine materials. Only between 120–200 cm and 270–384 cm were distinctly lower values typical of terrestrial material (up to −27.5‰) measured.

3.5. Pigments

The following pigments were studied: (1) chloropigments-a: Chlns-a (i.e., chlorophyll-a [Chl-a] and its derivatives: pheophorbides-a, pyropheophorbides-a, Chl-a-allomers, Chl-a-epimer, pheophytin-a, pheophytin-a-epimer, pyropheophytin-a, the sum of steryl chlorin esters) and CPPB-aE; (2) chlorophyll-b (Chl-b); (3) chlorophylls-c (Chls-c); and (4) cyanobacteria carotenoids (i.e., zeaxanthin, canthaxanthin, and echinenone).

The sum of chloropigments-a (ΣChlns-a) concentrations in the long core (384 cm), used in this paper as a productivity proxy, ranged from ~30 to ~130 nmol/g dry weight (d.w.). (Figure 3d). The ΣChlns-a content was higher and most variable in two sections of this core—from ~80 to ~220 cm and from ~320 to ~384 cm. The highest value was found in the 118- to 120-cm layer. In the short core (50 cm) ΣChlns-a concentrations ranged from ~40 to ~330 nmol/g d.w. (Figure 4b). Values were higher in the top 14 cm of
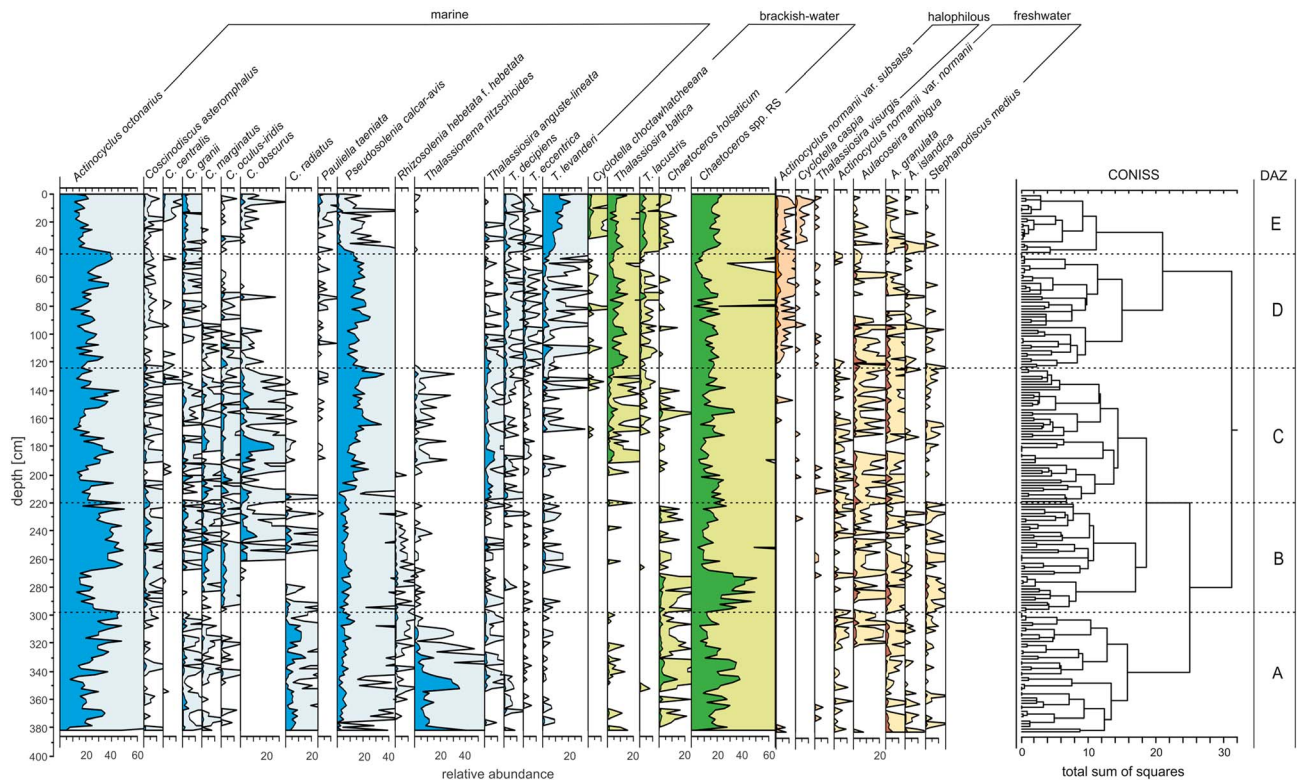
Figure 2. Diatom diagrams: Relative abundance of selected diatom taxa (darker color [%]; lighter color [‰]).

this core and lower in the layers from 14 to 50 cm. Comparison of the ΣChlns-a profiles in the long and short cores indicated that the uppermost section (~20 cm) of the long core had been lost during collection.

CPPB-aE, formed from pyropheophorbide-a (Louda et al., 2000), is much less stable under oxic conditions than is the sum of other chloropigments-a. Therefore, the CPPB-aE/ΣChlns-a ratio illustrates oxygen depletion in the near-bottom water (Szymczak-Żyła, 2018) and is tested in this paper as a new paleoredox proxy. The CPPB-aE/ΣChlns-a molar ratio in the long core ranged from ~0.04 to ~1.3 (Figure 5a). Values of CPPB-aE/ΣChlns-a were higher and most variable in two sections of this core—from ~80 to ~230 cm and from ~300 to ~384 cm. The highest values (>1.0) were found in the layers from ~112 to ~122 cm and in the lowermost section of this core—from ~370 to ~384. In the short core, CPPB-aE/ΣChlns-a ranged from ~0.02 to ~1.4. (Figure 4c). Values were higher in the top 14 cm section of the core and much lower in the layers from 14 to 50 cm (up to 0.35).

The concentrations of cyanobacteria marker carotenoids (zeaxanthin, canthaxanthin, and echinenone) in the long core are presented in Figures 6a–6c. They ranged from ~10 to ~50 (zeaxanthin), ~1.5 to ~8 (canthaxanthin), and ~1.5 to ~16 nmol/g d.w. (echinenone). The profiles of these three carotenoids were similar, and the concentrations were higher in two sections of this core—from ~80 to ~180 cm and from ~320 to ~384 cm. In the short core, concentrations of cyanobacteria marker carotenoids (Figures 4d–4f) ranged from ~10 to ~70 (zeaxanthin), ~1.5 to ~15 (canthaxanthin), and ~1.0 to ~10 nmol/g d.w. (echinenone). Distinctly higher values were found in the uppermost 12-cm-long section of the core.

The ratios of selected pigments characteristic for particular phytoplankton groups were used in this paper to trace past changes in phytoplankton composition. The Chls-c/Chl-a ratio indicated changes between organisms containing Chls-c (mainly diatoms but including chrysophytes and dinoflagellates) and other photosynthetic organisms. This ratio was higher in the uppermost 30 cm of the core and in the section from ~180 to ~320 cm (Figure 6e). The Chls-c/Chl-b ratio indicated changes between organisms containing Chls-c (mainly diatoms) and those containing Chl-b (mainly green algae). Higher values of this ratio were found in the core layers from ~200 to ~350 cm (Figure 6f). The echinenone to Chls-c ratio (Echin/Chls-c) was used to give an indication of cyanobacteria and organisms containing Chls-c (mainly diatoms)
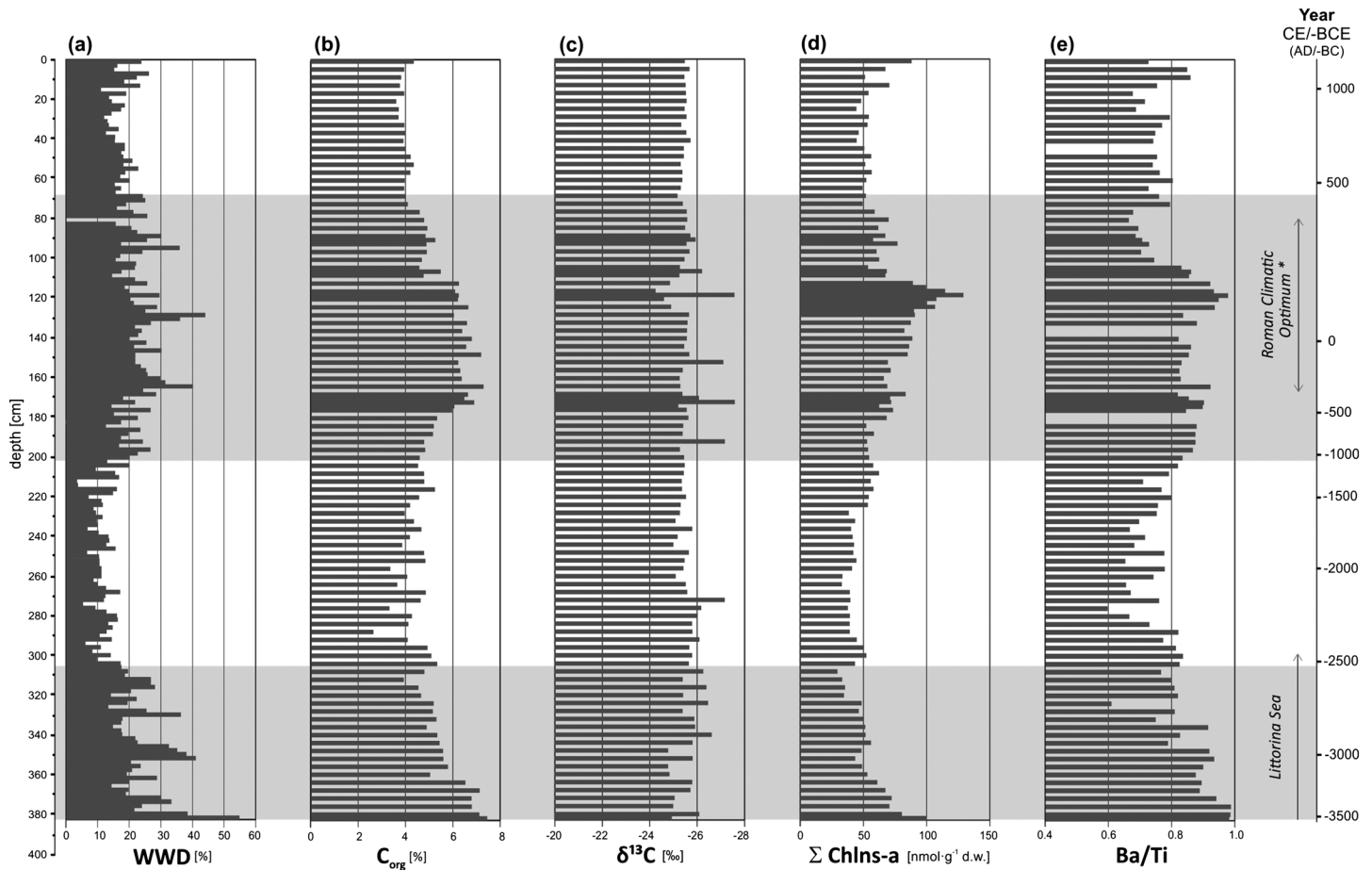
Figure 3. Proxy profiles for the long sediment core: (a) WWD = relative abundance of warm-water diatoms (%); (b) C_{org} = organic carbon (%); (c) $\delta^{13}C$ = stable organic carbon isotope ratio (‰); (d) ΣChlns-a = sum of chloropigments-a (nmol/g d.w.); (e) Ba/Ti = barium-to-titanium ratio. The gray areas indicate warm periods; * according to Hass (1996).
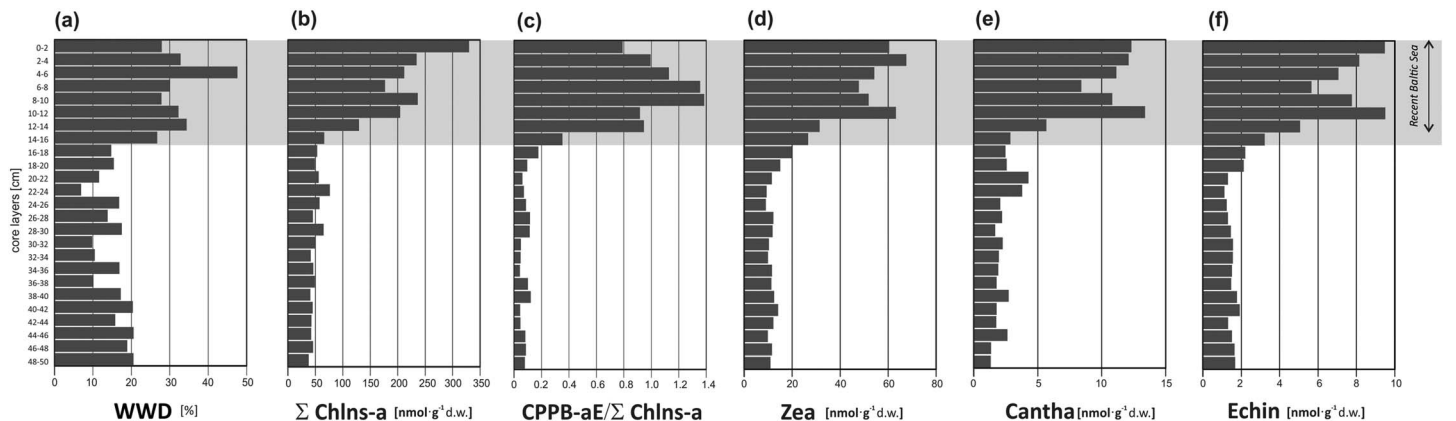
Figure 4. Proxy profiles for the short sediment core: (a) WWD = abundance of warm-water diatoms (%); (b) ΣChlns-a = sum of chloropigments-a (nmol/g d.w.); (c) CPPB-aE/ΣChlns-a = molar ratio of $13^2,17^3$-cyclopheophorbide-a enol to sum of chloropigments-a; (d) Zea = zeaxanthin (nmol/g d.w.); (e) Cantha = canthaxanthin (nmol/g d.w.); (f) Echin = echinenone (nmol/g d.w.). The gray areas indicate warm periods.
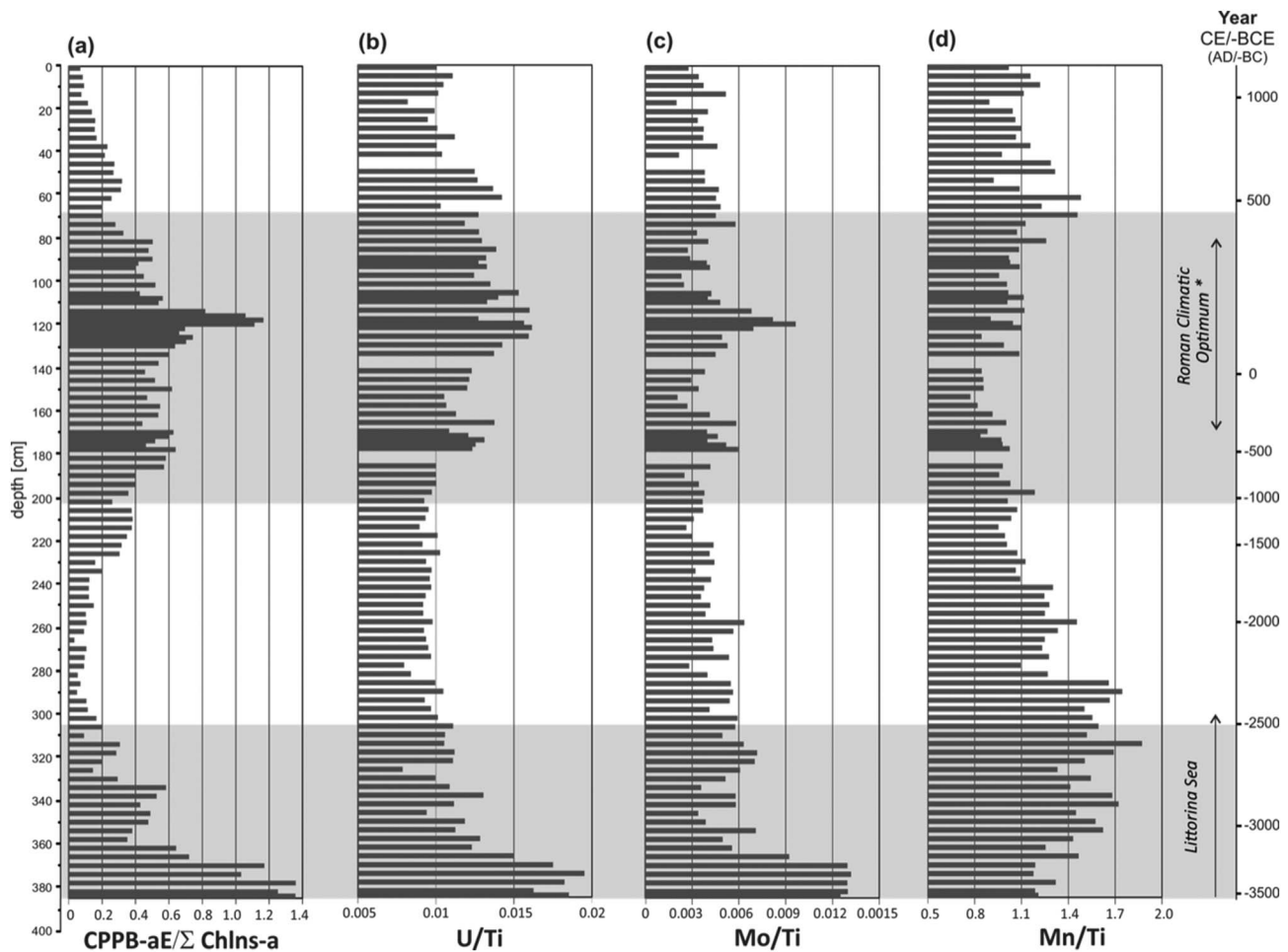
Figure 5. Proxy profiles for the long sediment core: (a) CPPB-aE/ΣChlns-a = molar ratio of $13^2,17^3$-cyclopheophorbide-a enol to the sum of chloropigments-a; (b) U/Ti = uranium-to-titanium ratio; (c) Mo/Ti = molybdenum-to-titanium ratio; (d) Mn/Ti = manganese-to-titanium ratio. The gray areas indicate warm periods; * according to Hass (1996).

proportion. Echinenone is more stable than Chls-c, but their ratio profile reflects cyanobacteria dominance. Values of Echin/Chls-c were higher in two sections of this core—from ~100 to ~220 cm and from ~300 to ~384 cm (Figure 6g).
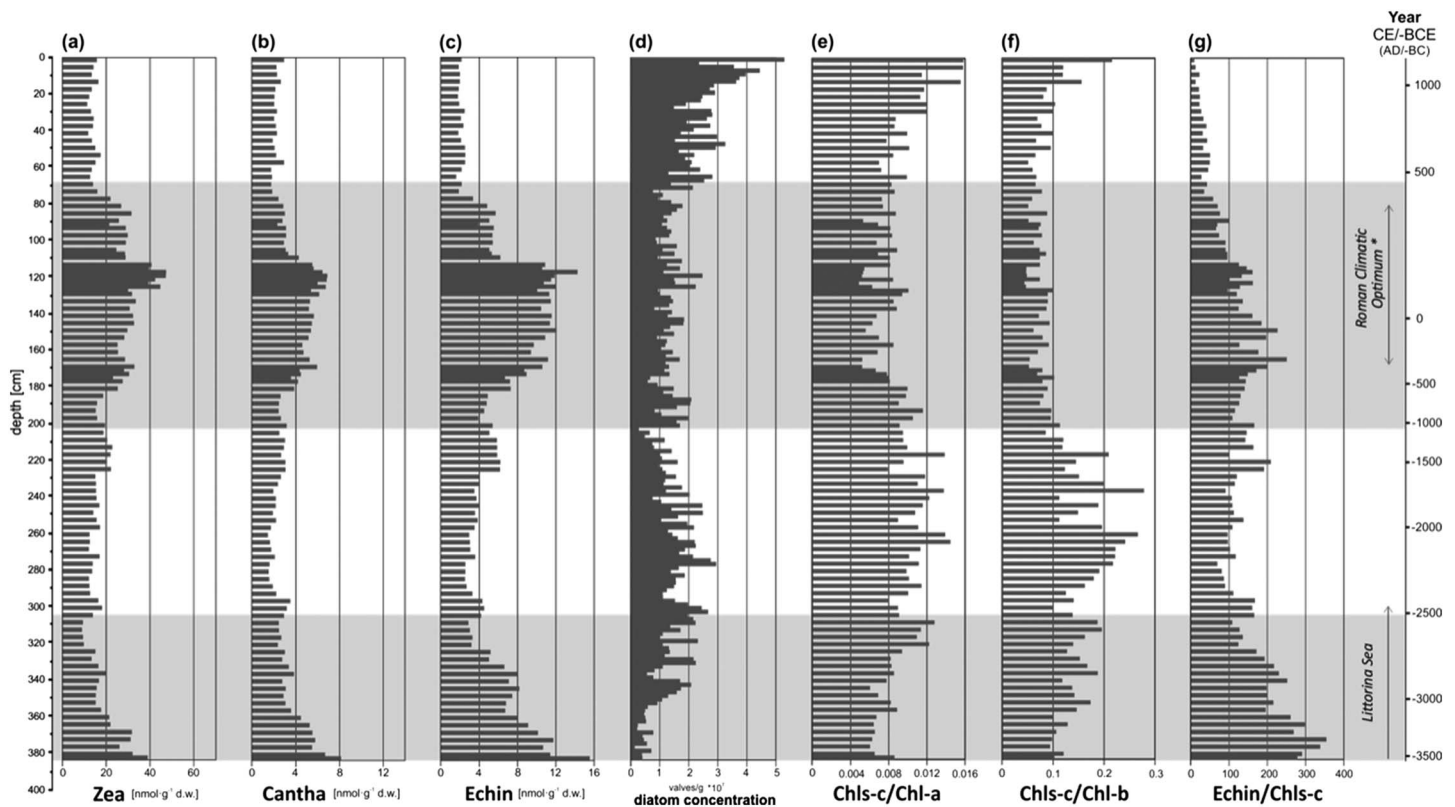
3.6. Metals

This paper focuses on metals that can be used for reconstructing changes in primary production level (i.e., Ba) and oxygen conditions (i.e., U, Mo, and Mn), as well as Ti, which was used as the normalizing factor. The profile of the Ba/Ti ratio (Figure 3e) indicates enrichment in Ba in two sections of this core—from ~100 to ~220 cm and from ~280 to ~384 cm. The U/Ti (Figure 5b) ratios are higher in the layers from ~50 to ~180 cm and from ~300 to ~384 cm. The Mo/Ti ratio profile (Figure 5c) indicates two maxima in the layers from ~112 to ~122 cm and from ~364 to ~384 cm. The profile of the Mn/Ti ratio (Figure 5d) points to enrichment in Mn in the sections from ~40 to ~80 cm and from ~240 to ~360 cm.

3.7. Statistical Analysis

The values of the autocorrelation function and partial autocorrelation function coefficients (Table S3 in the supporting information) show that only first lags for all parameters (except δ13C) are significant, and their positive value means that a high value of the parameter in the layer leads to their increase in the next layer. The augmented Dickey-Fuller test results for the null hypothesis of a unit root based on the components representation are presented in Table S4 in the supporting information. Our results show that all data-

AGU
100
ADVANCING EARTH
AND SPACE SCIENCE

Paleoceanography and Paleoclimatology

10.1029/2018PA003474

Figure 6. Proxy profiles for the long sediment cores: (a) Zea = zeaxanthin (nmol/g d.w.); (b) Cantha = canthaxanthin (nmol/g d.w.); (c) Echin = echinenone (nmol/g d.w.); (d) total diatom concentration (valves/g * 10^7); (e) Chls-c/Chl-a = molar ratio of chlorophylls-c to chlorophyll-a; (f) Chls-c/Chl-b = molar ratio of chlorophylls-c to chlorophyll-b; (g) Echin/Chls-c = molar ratio of echinenone to chlorophylls-c. The gray areas indicate warm periods; * according to Hass (1996).

generating processes include both a trend component and a cycle component (Table 1). The results of the cluster analysis including oxygen-deficiency proxies (CPPB-aE/$\sum$Chlns-a, U/Ti, and Mo/Ti) are presented in the Figure 7.

4. Discussion

4.1. Changes in Primary Production

The high concentration of the ΣChlns-a in the surface sediment layer (0–2 cm) of the short core (Figure 4b) indicates that present-day primary production in the Gulf of Gdańsk waters is high. This is consistent with studies on the trophic state of this basin (HELCOM, 2014; Łysiak-Pastuszak et al., 2013; Wasmund et al., 2001). The profile of ΣChlns-a in the short core (Figure 4b), which records the accumulation rate of the recent sediments (Szymczak-Żyła et al., 2017), suggests that high primary production has been occurring in this area for the last ca. 100 years. The depth-variable profile of ΣChlns-a concentration in the long core sediments formed during the last 5,500 years (Figure 3d) indicates that there may also have been high primary production periods in the past. A similar tendency observed for the organic carbon (C_{org}) content (Figure 3b), which is a widely used productivity proxy, confirms this. The positive, statistically significant correlation between the trend of ΣChlns-a concentration and C_{org} points to the similarity in both patterns ($R = 0.74$; $p < 0.05$; Table 1a). Thus, despite the instability of chloropigments-a, their sum is a good marker used for tracking changes in primary production level.

The lowermost part of the long core, with high ΣChlns-a and C_{org} contents, was formed before ca. 2500 BCE, during the Littorina Sea stage (Figures 3b and 3d). Thus, the results show a relatively high primary production in this period. A higher primary production in the Littorina Sea than in the preceding postglacial Baltic stages has also been reported by other authors (Andrén et al., 2000, Kostecki, 2015; Sohlenius et al., 1996, 2001). Andrén et al. (2000) and Sohlenius et al. (2001) reported increases of C_{org} in the Bornholm Basin

Table 1

Correlation Coefficients of the Trend and Cycle Components of Proxies Used for Reconstruction of Changes in Primary Production Level, Oxygen Conditions, and Phytoplankton Composition in the Gulf of Gdańsk

(a) Primary production

Variables	Time series components	C_{org}	ΣChlns-a	Ba/Ti	WWD
C_{org}	Trend	1			
	Cycle	1			
ΣChlns-a	Trend	**0.74**	1		
	Cycle	**0.34**	1		
Ba/Ti	Trend	**0.73**	**0.65**	1	
	Cycle	−0.03	−0.07	1	
WWD	Trend	**0.83**	**0.75**	**0.75**	1
	Cycle	0.04	0.00	0.07	1

(b) Oxygen conditions

		CPPB-aE/ΣChlns-a	U/Ti	Mo/Ti	Mn/Ti
CPPB-aE/ ΣChlns-a	Trend	1			
	Cycle	1			
U/Ti	Trend	**0.93**	1		
	Cycle	0.06	1		
Mo/Ti	Trend	**0.69**	**0.69**	1	
	Cycle	**0.21**	**0.37**	1	
Mn/Ti	Trend	**−0.36**	**−0.25**	0.25	1
	Cycle	−0.15	**0.34**	**0.35**	1

(c) Phytoplankton composition

		Zea	Cantha	Echin	Diatom concentration	Chls-c/Chl-a	Chls-c/Chl-b	Echin/Chls-c	WWD	CPPB-aE/ΣChlns-a
Zea	Trend	1								
	Cycle	1								
Cantha	Trend	**0.90**	1							
	Cycle	**0.80**	1							
Echin	Trend	**0.87**	**0.97**	1						
	Cycle	**0.83**	**0.77**	1						
Diatom concentration	Trend	**−0.42**	**−0.47**	**−0.61**	1					
	Cycle	0.14	0.08	0.13	1					
Chls-c/Chl-a	Trend	**−0.67**	**−0.69**	**−0.75**	**0.80**	1				
	Cycle	**−0.34**	**−0.29**	**−0.36**	−0.14	1				
Chls-c/Chl-b	Trend	**−0.63**	**−0.46**	**−0.40**	0.10	**0.58**	1			
	Cycle	**−0.21**	**−0.22**	−0.19	0.00	**0.62**	1			
Echin/Chls-c	Trend	**0.35**	**0.63**	**0.72**	**−0.79**	**−0.62**	0.13	1		
	Cycle	**0.41**	**0.44**	**0.55**	0.08	**−0.67**	**−0.43**	1		
WWD	Trend	**0.67**	**0.84**	**0.78**	**−0.37**	**−0.73**	**−0.56**	**0.56**	1	
	Cycle	−0.15	0.01	0.02	0.05	0.04	0.14	−0.18		
CPPB-aE/ ΣChlns-a	Trend	**0.84**	**0.88**	**0.86**	**−0.60**	**−0.83**	**−0.56**	**0.62**	**0.82**	1
	Cycle	**0.54**	**0.41**	**0.57**	0.06	**−0.29**	−0.14	**0.37**	−0.11	1

Note. Bold = significant; $p < 0.05$.

and Gotland Deep sediments formed during the Littorina Sea stage. The high ΣChlns-a and C_{org} contents in the Gulf of Gdańsk long core sediments at approximately 120 cm, which were formed during the Post-Littorina stage, between ~1000 BCE and ~400 CE (Figures 3b and 3d) can be related to the Roman Climatic Optimum. These ΣChlns-a and C_{org} profiles (Figures 3b and 3d) are very similar to those from the core taken in 2001 at a location close to the present sampling location (Szymczak-Żyła & Kowalewska, 2009). That core did not reflect the changes taking place during the Littorina Sea/Post-Littorina Sea transition, because it did not contain sediments older than 4,000 years. Nevertheless, the core sampled in 2001 displayed a significant increase in ΣChlns-a content in the Roman Climatic Optimum. The high primary production event recorded during the Post-Littorina Sea stage has been reported in other Baltic Sea
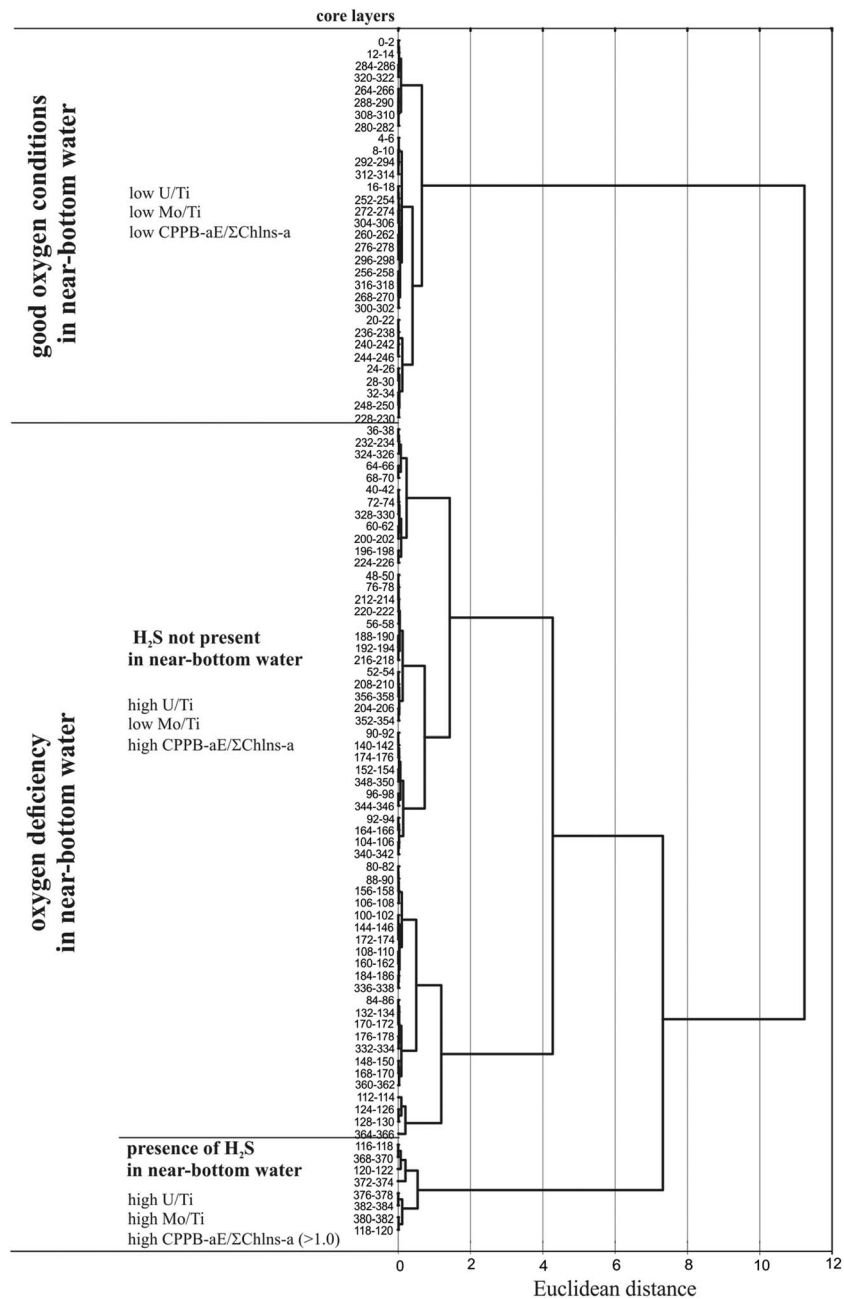
Figure 7. Results of cluster analysis including oxygen deficiency proxies (CPPB-aE/∑Chlns-a, U/Ti, and Mo/Ti): Hierarchical dendrogram of the long core layers (Ward′s method, Euclidean distance).

regions by other authors, but these authors observed it occurring during Medieval times. Dippner and Voss (2004) presented results for a sediment core from the Central Gotland Basin that showed high organic carbon content in sediments formed between 1160 and 1250 CE, indicating high primary production in that period. These results were confirmed by Harff et al. (2001), who measured a high level of organic carbon in the sediments formed at that time in the Gotland Basin, and by Funkey et al. (2014), who presented results for cores collected from the northern Gotland Basin and the Faro Deep, farther to the south. Our results show that the conditions giving rise to high primary production in the Gulf of Gdańsk could already have been prevailing in ancient Roman times and not just in Medieval times.

It can be assumed that the high content of ΣChlns-a and C_{org} in sediments may have resulted from the better preservation of organic matter under the reducing conditions that occurred at that time in the deeper Baltic

basins. However, Sohlenius et al. (2001) presented results indicating a high content of organic carbon in sediments from the Arkona and Bornholm Basins deposited in an environment that was oxic at that time. This indicates that organic carbon enrichment in Littorina Sea sediments was a question of higher productivity, not only of better preservation. Barium (Ba) enrichment in the sediments in the corresponding layers further support the concept of increased primary production in the Gulf of Gdańsk during the Littorina Sea stage and the Roman Climatic Optimum. Although Ba has proven to be a good indicator of paleoproductivity as it is taken up by sinking biogenic particles, its quantitative significance has been questioned (Sternbeck et al., 2000; Tribovillard et al., 2006). This proxy suffers from the fact that under reducing conditions, Ba is solubilized and thus released from sediments to the water column and high primary production periods may develop without Ba enrichment in the sediments. However, in contrast to the above, the Ba/Ti profile (Figure 3e) indicates enrichment in the core sections with higher ΣChlns-a and C_{org} contents. This is supported by the positive, statistically significant correlation between the trend component of Ba/Ti and ΣChlns-a ($R = 0.65$; $p < 0.05$; Table 1a) and between Ba/Ti and C_{org} ($R = 0.73$; $p < 0.05$; Table 1a). This confirms the high primary production events in the Gulf of Gdańsk during the Littorina Sea stage and the Roman Climatic Optimum. The positive, statistically significant correlations with the productivity proxies (ΣChlns-a, C_{org}, and Ba/Ti) and the percentage of warm-water-preferring diatoms (WWD; Table 1a) indicate that high primary production events were most probably elicited by climate warming.

The decrease in ΣChlns-a and C_{org} contents in sediments observed at the beginning of the Post-Littorina Sea stage (Figures 3b and 3d) may indicate a decrease in primary production in the Gulf of Gdańsk area. During that time, the reduction in depth of the Danish Straits led to a salinity decrease, agreeing with the δ^{13}C profile (Figure 3c), where we can observe a decrease of δ^{13}C values and frequent maxima, most probably indicating higher allochthonous organic matter input from the River Vistula. The occurrence of cold-water species such as *Coscinodiscus marginatus*, *C. oculus-iridis*, and *Rhizosolenia hebetata* f. *hebetata* (Figure 2) is a clear indication of the lower water temperature resulting from the cooler climate of the late Subboreal and Subatlantic chronozones. At the same time, warm-water plankton, that is, *C. radiatus*, almost completely disappeared and the percentage of warm-water-preferring diatoms decreased (Figure 3a). The increase in the number of resting spores of *Chaetoceros* spp. (Figure 2) also signifies unpropitious conditions at that time, that is, nutrient depletion and/or low temperature. In addition, lower Ba/Ti values indicate lower primary production in this period (Figure 3e).

4.2. Oxygen Condition Reconstruction

The increase in C_{org} and ΣChlns-a in deeper layers of the long sediment core (Figures 3b and 3d) provides evidence for a high past primary production, but it can also be an effect of the better preservation of organic matter due to poorer oxygen concentrations in the near-bottom water. Identification of past hypoxic/anoxic periods is therefore very important, especially in the context of climate change studies. The presence of laminated layers in the sediment record and trace element distributions (e.g., U, Mo, and Mn) are the main methods currently used for this purpose, although they do not always produce conclusive results (Tribovillard et al., 2006; Zillén et al., 2008). A study of recent Gulf of Gdańsk sediments showed that also a labile degradation product of Chl-a, CPPB-aE, in sediments may be a marker of oxygen deficiency in near-bottom water (Szymczak-Żyła, 2018). The high ratio of this derivative to the sum of other chloropigments-a (CPPB-aE/ΣChlns-a) in recent sediments indicated a significant deterioration of the oxygen conditions in the near-bottom water. The profile of CPPB-aE/ΣChlns-a ratio in the short sediment core (Figure 4c) showed that oxygen concentration in the near-bottom water and sediments has been decreasing since the beginning of the twentieth century, which is consistent with the literature data (Cyberska & Lauer, 1990). The highest values of the CPPB-aE/ΣChlns-a ratio (>1.0; Figure 4c) were found in the layers that formed when hydrogen sulfide was recorded in the Gdańsk Deep.

The CPPB-aE/ΣChlns-a profile in the long sediment core showed an increase of this ratio in two parts of the core (Figure 5a): in sediment layers of the lowermost part of the core, formed before ca. 2500 BCE (Littorina Sea stage) and during the Roman Climatic Optimum. Analysis of the profiles of the elements used as paleoredox proxies (Figures 5b–5d) shows that the sediments from these two sections are enriched in uranium (U/Ti in Figure 5b). This trace metal is enriched in sediments under oxygen-depleted conditions (Tribovillard et al., 2006). The positive, statistically significant correlation between the trend component of CPPB-aE/ΣChlns-a and U/Ti points to the considerable similarity in both patterns ($R = 0.93$; $p < 0.05$; Table 1b).

The combined use of U and Mo enrichments may also enable suboxic environments to be distinguished from euxinic (sulfidic) ones (Tribovillard et al., 2006). U is enriched in sediments deposited under reducing conditions, whereas Mo (euxinia proxy) is enriched in sediments formed in the presence of hydrogen sulfide in the near-bottom water. Analysis of the Mo/Ti profile in the long sediment core (Figure 5c) shows that Mo/Ti values are highest in the sediment layers in which the CPPB-aE/ΣChlns-a ratio reached maximum values (Figure 5a). Cluster analysis including oxygen deficiency proxies (CPPB-aE/∑Chlns-a, U/Ti, and Mo/Ti) revealed that high values of CPPB-aE/ΣChlns-a ratio (>1.0) may indicate the presence of hydrogen sulfide in the near-bottom water (Figure 7).

The CPPB-aE/ΣChlns-a profile in the long sediment core showed an improvement in oxic conditions at the beginning of the Post-Littorina Sea stage (Figure 5a). The CPPB-aE/ΣChlns-a ratio in the layers from ~2500 to 1500 BCE is significantly lower, which suggests good oxygen conditions in the near-bottom water. This sediment section is also characterized by high Mn/Ti ratio (Figure 5d). Enrichment in Mn is used as a proxy for bottom water oxygenation (Naeher et al., 2013; Neumann et al., 1997). These observations indicate that the CPPB-aE/ΣChlns-a ratio is a good, new oxygen-deficiency proxy that can be used to reconstruct not only oxygen conditions but also the presence of hydrogen sulfide during sediment formation.

4.3. Cyanobacteria Blooms

Cyanobacteria blooms, which are expanding nowadays worldwide in coastal zones, estuaries, and lakes, are attributed to anthropogenic nutrient input and climate change (Cook et al., 2016; Paerl, 1988; Paerl & Huisman, 2008, 2009). These blooms, especially of the toxic heterocystous species *Nodularia spumigena*, are a sign of eutrophication and are a serious problem of the contemporary Baltic Sea (Henricksen, 2005; Mazur-Marzec et al., 2013; Stal et al., 2003). The study on recent sediments from the Gulf of Gdańsk indicated that the marker carotenoids of cyanobacteria in the surface sediments were zeaxanthin, canthaxanthin, and echinenone (Krajewska et al., 2019). The results of that paper showed that canthaxanthin is a marker of heterocystous cyanobacteria species, which can form toxic blooms in the Baltic. Zeaxanthin most probably originated mainly from pico-cyanobacteria and micro-cyanobacteria. Echinenone occurs in both filamentous and noncolonial cyanobacteria and may be used as a universal cyanobacteria proxy (Krajewska et al., 2019).

In the present work, the cyanobacteria marker carotenoid profiles in the short and long sediment cores revealed three main maxima indicating a high cyanobacteria abundance: The first one was formed during the Littorina Sea stage (i.e., before ca. 2500 BCE), the second between ca. 500 BCE and 400 CE (around the Roman Climatic Optimum; Figures 6a–6c), and the third one during the last 100 years (Figure 4d–4f). Moreover, the high concentrations of canthaxanthin in these sediment sections indicate that blooms of heterocystous cyanobacteria occurring in past millennia were likely as intensive as nowadays. Also, chemical and genetic analyses of the same long core samples found hepatotoxic nodularins specific to *N. spumigena* occurrence in deep sediments, which were present in the highest concentrations during the Roman Climatic Optimum (Cegłowska et al., 2018). The results of that work demonstrate that these were the same two subpopulations of this species as those occurring nowadays. The inference regarding heterocystous cyanobacteria blooms occurring in past millennia is also consistent with the results of glycolipid studies on long sediment cores from the Baltic's Gotland Basin (Sollai et al., 2017), which revealed the presence of heterocystous cyanobacteria in deep sediments, the proportion of *Nodularia* sp. being the highest. Cyanobacteria proxies were also identified in deep sediment cores collected from the Baltic by other authors (Bianchi et al., 2000; Funkey et al., 2014). However, the authors of these papers treated zeaxanthin, considered a universal marker of cyanobacteria in aquatic basins and their sediments (Jeffrey et al., 1997), as the best sedimentary marker of cyanobacteria. Echinenone was also recorded but in smaller amounts than zeaxanthin (Funkey et al., 2014).

Cyanobacteria abundance in the Gulf of Gdańsk is correlated with the oxygen deficiency in the near-bottom water occurring in those periods (Figure 5a). The positive, statistically significant correlations between the trend component of cyanobacteria marker carotenoids and CPPB-aE/ΣChlns-a ratio point to the similarity in the patterns (Table 1c). This was also observed by other authors studying sediment cores from other Baltic Sea regions (Bianchi et al., 2000; Funkey et al., 2014). These authors suggested that cyanobacteria were abundant already during the Littorina Sea stage (7,000–4,000 BP), when hypoxia caused by stratification of the water column stimulated the release of phosphorus from sediments into the seawater, creating

conditions ideal for N_2-fixing cyanobacteria. According to Bianchi et al. (2000), such a situation probably caused the limiting nutrient to change from nitrogen to phosphorus, a situation unfavorable to diatoms. This is corroborated by our diatom results. Namely, the concentration of diatoms in the lowermost part of the long core (384–340 cm, Figure 6d), despite the high productivity (high C_{org} and ΣChlns-a, Figures 3b and 3d), was lower than that during the later stages of the Baltic Sea. A low diatom abundance during the Littorina Sea stage was also reported by other authors (Andrén et al., 2000). Around 4500 BP, the reduction in depth of the Danish Straits improved oxygen conditions in the Gdańsk Basin, indicated by low values of CPPB-aE/ΣChlns-a (Figure 5a), making conditions less favorable for cyanobacteria growth. The diatom concentration was higher in that period than during the Littorina Sea stage (Figure 6d). This is backed up by the increase in the Chls-c/Chl-a and Chls-c/Chl-b ratios (Figures 6e and 6f) and confirmed by the negative, statistically significant correlation between the CPPB-aE/ΣChlns-a ratio and Chls-c/Chl-a and Chls-c/Chl-b ratios (Table 1c). Chls-c are less stable than Chl-a and Chl-b (Leavitt & Hodgson, 2001), so the increase in these ratios provides evidence for the higher ratio of organisms containing Chls-c (mainly diatoms) to other photosynthetic organisms than in the Littorina Sea. The Echin/Chls-c ratio indicates a lower ratio of cyanobacteria to diatoms in that period (Figure 6g and Table 1c).

The profiles of cyanobacteria marker carotenoids (Figures 6a–6c) are similar to the percentages of planktic WWD (Figure 3a). The positive, statistically significant correlations between the trend component of cyanobacteria marker carotenoid concentrations and WWD point to the similarity in the patterns (Table 1c), especially for the canthaxanthin and WWD ($R = 0.84$; $p < 0.05$; Table 1c). This suggests that heterocystous cyanobacteria blooms accompanied climate warming, obviously as long as sufficient concentrations of necessary nutrients were available. Cyanobacteria tend to develop at higher temperatures (Paerl & Huisman, 2008, 2009; Stal, 2009). *N. spumigena*, the most abundant heterocystous cyanobacteria species forming present-day blooms in the Baltic, requires temperatures ≥15 °C, high levels of solar irradiation, and calm water (Henricksen, 2005; Stal et al., 2003). Such conditions prevailed during the Roman Climatic Optimum—at least, that was the situation in ancient Rome, since no historical data older than 1,000 years is available from the southern Baltic coastal region (Kowalewska, 2001), and early human settlement was minimal there.

5. Conclusions

There were high primary production periods during the Littorina Sea stage (before ca. 2,500 BCE) and the Roman Climatic Optimum (between ca. 500 BCE and 400 CE). This was most probably caused by climate warming at favorable nutrient and hydrological conditions. Conditions favoring high levels of primary production occurred in the Gulf of Gdańsk already in ancient Roman times and not just in Medieval times, as shown for other parts of the Baltic Sea. The chloropigment-a maxima in the core sediments correspond to warm periods. The pigments were preserved as a result of favorable postdepositional conditions, namely, oxygen deficiency in the near-bottom water. The high levels of CPPB-aE/ΣChlns-a found in these layers of the sediment core confirm that oxygen was deficient in the near-bottom water during those periods, while high CPPB-aE/ΣChlns-a (>1.0) points to the occurrence of euxinia. The CPPB-aE/ΣChlns-a ratio is a good, new oxygen-deficiency proxy that can be used to reconstruct oxygen conditions in the near-bottom water. Heterocystous cyanobacteria blooms also occurred during past maximum primary production periods in the Littorina Sea and the Roman Climatic Optimum and were comparable to those occurring in the recent Baltic Sea, that is, within the last 100 years. Heterocystous cyanobacteria blooms accompanied climate warming in the Gulf of Gdańsk. Hence, eutrophication must also have occurred in the past, which means that natural factors also have substantial influences.

References

Ambio (1990). Special issue: Marine eutrophication. ISSN: 0044-7447, 19(3).

Andrén, E., Andrén, T., & Kunzendorf, H. (2000). Holocene history of the Baltic Sea as a background for assessing records of human impact in the sediment of the Gotland Basin. *The Holocene*, *10*(6), 687–702. https://doi.org/10.1191/09596830094944

Ardelan, M. V., Steinnes, E., Lierhagen, S., & Linde, S. O. (2009). Effects of experimental CO_2 leakage on solubility and transport of seven trace metals in seawater and sediment. *The Sciences of the Total Environment*, *407*(24), 6255–6266. https://doi.org/10.1016/j.scitotenv.2009.09.004

Battarbee, R. W. (1986). The eutrophication of Lough Erne inferred from changes in the diatom assemblages of [210]Pb- and ^{137}Cs-dated sediment cores. *Proceedings-Royal Irish Academy, Section B*, *86B*(6), 141–168.

Bianchi, T. S., Engelhaupt, E., Westmaan, P., Andrén, T., Rolff, C., & Elmgren, R. (2000). Cyanobacterial blooms in the Baltic Sea: Natural or human-induced? *Limnology and Oceanography: Methods*, *45*(3), 716–726. https://doi.org/10.4319/lo.2000.45.3.0716

Bodén, P. (1991). Reproducibility in the random settling method for quantitative diatom analysis. *Micropaleontology*, *37*(3), 313–319. https://doi.org/10.2307/1485893

Brock, F., Higham, T., Ditchfield, P., & Bronk Ramsey, C. (2010). Current pretreatment methods for AMS radiocarbon dating at Oxford Radiocarbon Accelerator Unit (ORAU). *Radiocarbon*, *52*(01), 103–112. https://doi.org/10.1017/S0033822200045069

Carpenter, E. J., O'Neil, J. M., Dawson, R., Capone, D. G., Siddiqui, P. J. A., Roenneberg, T., & Bergman, B. (1993). The tropical diazotrophic phytoplankter *Trichodesmium*: Biological characteristics of two common species. *Marine Ecology Progress Series*, *95*, 295–304. https://doi.org/10.3354/meps095295

Cegłowska, M., Toruńska-Sitarz, A., Kowalewska, G., & Mazur-Marzec, H. (2018). Specific chemical and genetic markers revealed a thousands-year presence of toxic Nodularia spumigena in the Baltic Sea. *Marine Drugs*, *16*(4), 116. https://doi.org/10.3390/md16040116

Chang, F. Y., Kao, S. J., & Liu, K. K. (1991). Analysis of organic and carbonate carbon in sediments. *Acta Oceanographica Taiwanica*, *27*, 14–150.

Conley, D. J., Björck, S., Bonsdorff, E., Carstensen, J., Destouni, G., Gustafsson, B. G., et al. (2009). Hypoxia-related processes in the Baltic Sea. *Environmental Science & Technology*, *43*(10), 3412–3420. https://doi.org/10.1021/es802762a

Conley, D. J., Cartensen, J., Aigars, J., Axe, P., Bonsdorff, E., Eremina, T., et al. (2011). Hypoxia is increasing in the coastal zone of the Baltic Sea. *Environmental Science & Technology*, *45*(16), 6777–6783. https://doi.org/10.1021/es201212r

Cook, P. L. M., Jennings, M., Holland, D. P., Beardall, J., Briles, C., Zawadzki, A., et al. (2016). Blooms of cyanobacteria in a temperate Australian lagoon system post and prior to European settlement. *Biogeosciences*, *13*(12), 3677–3686. https://doi.org/10.5194/bg-13-3677-2016

Cyberska, B., & Lauer, Z. (1990). Oxygen and thermohaline conditions in the Polish fishing zone in 1979–1983. *Oceanologia*, *29*, 3–25.

Dickey, D. A., & Fuller, W. A. (1979). Distribution of the estimators for autoregressive time series with a unit root. *Journal of the American Statistical Association*, *74*(74), 427–431.

Dippner, J. W., & Voss, M. (2004). Climate reconstruction of the MWP in the Baltic Sea areas based on biogeochemical proxies from a sediment record. *Baltica*, *17*(1), 5–16.

EC (2000). Directive of the European Parliament and the Council 2000/60/EC establishing a framework for community action in the field of water policy. *O J L*, *32*, 1–72.

EC (2008). Directive 2008/56/EC of the European Parliament and the Council of 17 June 2008 on establishing a framework for community action in the field of marine policy (marine strategy framework directive). *O J L*, *164*, 19–40.

Fuller, W. A. (2009). *Introduction to statistical time series*, (Vol. 428). New York: John Wiley & Sons.

Funkey, C. P., Conley, D. J., Reuss, N., Humborg, C., Jilbert, T., & Slomp, C. P. (2014). Hypoxia sustains cyanobacteria blooms in the Baltic Sea. *Environmental Science & Technology*, *48*(5), 2598–2602. https://doi.org/10.1021/es404395a

Goslar, T., Czernik, J., & Goslar, E. (2004). Low-energy ^{14}C AMS in Poznan Radiocarbon Laboratory, Poland. *Nuclear Instruments and Methods in Physics Research B*, *223-224*, 5–11. https://doi.org/10.1016/j.nimb.2004.04.005

Goslar, T., van der Knaap, W. O., van Leeuwen, J., & Kamenik, C. (2009). Free-shape ^{14}C age-depth modelling of an intensively dated modern peat profile. *Journal of Quaternary Science*, *24*(5), 481–499. https://doi.org/10.1002/jqs.1283

Håkansson, H. (2002). A compilation and evaluation of species in the general *Stephanodiscus, Cyclostephanos* and *Cyclotella* with a new genus in the family *Stephanodiscaceae*. *Diatom Research*, *17*(1), 1–139. https://doi.org/10.1080/0269249X.2002.9705534

Harff, J., Bohling, G., Davis, J. C., Endler, R., Kunzendorf, H., Olea, R. A., et al. (2001). Physico-chemical stratigraphy of Gotland Basin Holocene sediments, the Baltic Sea. *Baltica*, *14*(1), 58–66.

Hasle, G. R., & Syvertsen, E. E. (1996). Marine diatoms. In C. R. Tomas (Ed.), *Identifying marine diatoms and dinoflagellates* (pp. 5–385). San Diego: Academic Press.

Hass, H. C. (1996). Northern Europe climate variations during late Holocene: Evidence from marine Skagerrak. *Palaeogeography, Palaeoclimatology, Palaeoecology*, *123*(1–4), 121–145. https://doi.org/10.1016/0031-0182(95)00114-X

Hedges, J. I., & Stern, J. H. (1984). Carbon and nitrogen determinations of carbonate containing solids. *Limnology and Oceanography*, *29*(3), 657–663. https://doi.org/0.4319/lo.1984.29.3.0657

HELCOM (2007). Activities 2006. Overview. Baltic Sea Environment Proceedings No. 112.

HELCOM (2009). Eutrophication in the Baltic Sea. An integrated thematic assessment of the effects of nutrient enrichment in the Baltic Sea region. Baltic Sea Environment Proceedings No. 115B.

HELCOM (2013). Climate change in the Baltic Sea Area HELCOM thematic assessment in 2013. Baltic Sea Environment Proceedings No. 137.

HELCOM (2014). Eutrophication status of the Baltic Sea 2007-2011. A concise thematic assessment. Baltic Sea Environment Proceedings No. 143.

Henricksen, P. (2005). Estimating nodularin content of cyanobacterial blooms from abundance of *Nodularia spumigena* and its characteristic pigments—A case study from the Baltic entrance area. *Harmful Algae*, *4*(1), 167–178. https://doi.org/10.1016/j.hal.2004.02.003

Jeffrey, S. W., Mantoura, R. F. C., & Wright, S. W. (Eds) (1997). *Phytoplankton pigments in oceanography*. Paris: SCOR- UNESCO Publishing.

Kabel, K., Moros, M., Porsche, C., Neumann, T., Adolphi, F., Andersen, T. J., et al. (2012). Impact of climate change on the Baltic Sea ecosystem over the past 1,000 years. *Nature Climate Change*, *2*(12), 871–874. https://doi.org/10.1038/nclimate1595

Kigoshi, K., Suzuki, N., & Shiraki, M. (1980). Soil dating by fractional extraction of humic acid. *Radiocarbon*, *22*(03), 853–857. https://doi.org/10.1017/S0033822200010237

Kostecki, R. (2015). Age and evolution of the Littorina Sea in the light of geochemical analysis and radiocarbon dating sediment of cores from the Arkona Basin and Mecklenburg Bay (SW Baltic Sea). *Landform Analysis*, *29*, 27–33. https://doi.org/10.12657/landfana.029.004

Kowalewska, G. (2001). Algal pigments in Baltic sediments as markers of ecosystem and climate changes. *Climate Research*, *18*(1–2), 89–96. https://doi.org/10.3354/cr018089

Kowalewska, G., Winterhalter, B., & Konat, J. (1998). Chlorophyll a and its derivatives in deep Baltic sediments. *Oceanologia*, *40*(1), 65–69.

Kowalewska, G., Winterhalter, B., Talbot, H. M., Maxwell, J. R., & Konat, J. (1999). Chlorins in sediments of the Gotland Deep (Baltic Sea). *Oceanologia*, *41*(1), 81–97.

Krajewska, M., Szymczak-Żyła, M., Kobos, J., Witak, M., & Kowalewska, G. (2019). Canthaxanthin in recent sediments as an indicator of heterocysteous cyanobacteria in coastal waters. *Oceanologia*, *61*(1), 78–88. https://doi.org/10.1016/j.oceano.2018.07.002

Krajewska, M., Szymczak-Żyła, M., & Kowalewska, G. (2017). Carotenoid determination in recent marine sediments—Practical problems during sample preparation and HPLC analysis. *Current Chemistry Letters*, *6*, 91–104. https://doi.org/10.5267/j.ccl.2017.4.003

Kramarska, R., Smagała, S., & Uścinowicz, S. (1996). *Analiza porównawcza wyników uziarnienia osadów przy zastosowaniu laserowego miernika*. Gdańsk: Analysette 22. Archiwum OGM PIG-PIB. [in Polish].

Krammer, K., & Lange-Bertalot, H. (1986). Bacillariophyceae. 1. Teil: Naviculaceae. In H. Ettl, J. Gerloff, H. Heynig, & D. Mollenhauer (Eds.), *Süsswasser flora von Mitteleuropa, Band 2/1* (pp. 1–876). Stuttgart, New York: Gustav Fischer Verlag.

Krammer, K., & Lange-Bertalot, H. (1988). Bacillariophyceae. 2. Teil: Bacillariaceae, Epithemiaceae, Surirellaceae. In H. Ettl, J. Gerloff, H. Heynig, & D. Mollenhauer (Eds.), *Süsswasserflora von Mitteleuropa, Band 2/2* (pp. 1–596). Jena: VEB Gustav Fischer Verlag.

Krammer, K., & Lange-Bertalot, H. (1991a). Bacillariophyceae. 3. Teil: Centrales, Fragilariaceae, Eunotiaceae. In H. Ettl, J. Gerloff, H. Heynig, & D. Mollenhauer (Eds.), *Süsswasserflora von Mitteleuropa, Band 2/3* (pp. 1–576). Stuttgart, Jena: Gustav Fischer Verlag.

Krammer, K., & Lange-Bertalot, H. (1991b). Bacillariophyceae. 4. Teil: Achnanthaceae, Kritische Ergänzungen zu Navicula (Lineolatae) und Gomphonema, Gesamtliteraturverzeichnis Teil 1-4. In H. Ettl, J. Gerloff, H. Heynig, & D. Mollenhauer (Eds.), *Süsswasserflora von Mitteleuropa, Band 2/4*, (pp. 1–437). Stuttgart, Jena: Gustav Fischer Verlag.

Kristiansen, S. M., Dalsgaard, K., Holst, M. K., Aaby, B., & Heinemeier, J. (2003). Dating of prehistoric burial mounds by 14C analysis of soil organic matter fractions. *Radiocarbon*, *45*(1), 101–112. https://doi.org/10.1017/S0033822200032434

Leavitt, P. R., & Hodgson, D. A. (2001). Sedimentary pigments. In J. P. Smol, J. B. Birks, & W. M. Last (Eds.), *Tracking trends environmental changes using lake sediments* (pp. 295–325). Dordrecht: Kluwer Academy Publisher.

Louda, J. W., Loitz, J. W., Rudnick, D. T., & Baker, E. W. (2000). Early diagenetic alteration of chlorophyll-a and bacteriochlorophyll-a in a contemporaneous marl ecosystem. *Organic Geochemistry*, *31*(12), 1561–1580. https://doi.org/10.1016/S0146-6380(00)00071-1

Łysiak-Pastuszak, E., Kraśniewski, W., & Saniewski, M. (2013). Ocena stanu eutrofizacji środowiska morskiego (Eutrophication assessment). In E. Jakusik et al. (Eds.), *Bałtyk Południowy w 2012 r. Charakterystyka wybranych elementów środowiska* (Southern Baltic Sea. Environmental conditions in 2012) (in Polish, summary in English). Gdynia, Warszawa: IMGW.

Majewski, A. (1990). Morfometria i hydrografia zlewiska. In A. Majewski (Ed.), *Zatoka Gdańska*, (pp. 10–19). Warszawa: IMGW, Wydawnictwa Geologiczne.

Matthäus, W., Nehring, D., Feistel, R., Nausch, G., Mohrholz, V., & Lass, H. U. (2008). The inflow of highly saline water into the Baltic Sea. In R. Feistel, G. Nausch, & N. Wasmund (Eds.), *State and evolution of the Baltic Sea, 1952–2005: A detailed 50-year survey of meteorology and climate, physics, chemistry, biology, and marine environment*, (pp. 265–309). Hoboken: John Wiley & Sons. https://doi.org/10.1002/9780470283134.ch10

Mayer, J. H., Burr, G. S., & Holiday, V. T. (2008). Comparisons and interpretations of charcoal and organic matter radiocarbon ages from buried soils in north-central Colorado, USA. *Radiocarbon*, *50*(3), 331–346. https://doi.org/10.1017/S0033822200053479

Mazur-Marzec, H., Sutryk, K., Kobos, J., Hebel, A., Hohlfeld, N., Błaszczyk, A., Toruńska, A., et al. (2013). Occurence of cyanobacteria and cyanotoxin in the southern Baltic proper. Filamentous cyanobacteria versus single-celled picocyanobacteria. *Hydrobiologia*, *701*(1), 235–252. https://doi.org/10.1007/s10750-012-1278-7

Naeher, S., Gilli, A., North, R. P., Hamann, Y., & Schubert, C. J. (2013). Tracing bottom water oxygenation with sedimentary Mn/Fe ratios in Lake Zurich, Switzerland. *Chemical Geology*, *352*, 125–133. https://doi.org/10.1016/j.chemgeo.2013.06.006

Neumann, T., Christiansen, C., Clasen, S., Emeis, K.-C., & Kunzendorf, H. (1997). Geochemical records of salt-water inflows into the deep basins of the Baltic Sea. *Continental Shelf Research*, *17*(1), 95–115. https://doi.org/10.1016/0278-4343(96)00023-4

Orive, E., Elliott, M., & de Jonge V. N. (Eds.) (2002). *Nutrients and eutrophication in estuaries and coastal waters. Proceedings of the 31st Symposium of the Estuarine and Coastal Sciences Association (ECSA), Held in Bilbao, Spain, 3–7 July 2000*, Dordrecht: Kluwer Academic Publishers.

Paerl, H. W. (1988). Nuisance phytoplankton blooms in coastal, estuarine, and inland waters. *Limnology and Oceanography*, *33*(4), 823–843. https://doi.org/10.4319/lo.1988.33.4part2.0823

Paerl, H. W., & Huisman, J. (2008). Climate: Blooms like it hot. *Science*, *320*(5872), 57–58. https://doi.org/10.1126/science.1155398

Paerl, H. W., & Huisman, J. (2009). Climate change: A catalyst for global expansion of harmful cyanobacterial blooms. *Environmental Microbiology Reports*, *1*(1), 27–37. https://doi.org/10.1111/j.1758-2229.2008.00004.x

Pountanen, E.-L., & Nikkilä, K. (2001). Carotenoid pigments as tracers of cyanobacterial blooms in recent and post-glacial sediments of the Baltic Sea. *Ambio*, *30*(4), 179–183. https://doi.org/10.1579/0044-7447-30.4.179

Reimer, P. J., Bard, E., Bayliss, A., Beck, J. W., Blackwell, P. G., Bronk Ramsey, C., et al. (2013). IntCal13 and Marine13 radiocarbon age calibration curves 0–50,000 years cal BP. *Radiocarbon*, *55*(04), 1869–1887. https://doi.org/10.2458/azu_js_rc.55.16947

Schrader, H., & Gersonde, R. (1978). Diatoms and silicoflagellates in the eight meters sections of the lower Pleistocene at Capo Rossello. *Utrecht Micropaleontological Bulletin*, *17*, 129–176.

Shepard, F. P. (1954). Nomenclature based on sand-silt-clay ratio. *Journal of Sedimentary Petrology*, *24*(3), 151–158.

Sohlenius, G., Emis, K.-C., Andrén, E., Andrén, T., & Kohly, A. (2001). Development of anoxia during the Holocene fresh-brackish water transition in the Baltic Sea. *Marine Geology*, *177*(3–4), 221–242. https://doi.org/10.1016/S0025-3227(01)00174-8

Sohlenius, G., Sternbeck, J., Andrén, E., & Westman, P. (1996). Holocene history of the Baltic Sea as recorded in a sediment core from the Gotland Deep. *Marine Geology*, *134*(3–4), 183–201. https://doi.org/10.1016/0025-3227(96)00047-3

Sollai, M., Hopmans, E. C., Bale, N. J., Mets, A., Warden, L., Moros, M., & Sinninghe Damsté, J. S. (2017). The Holocene sedimentary record of cyanobacterial glycolipids in the Baltic Sea: An evaluation of their application as tracers of past nitrogen fixation. *Biogeosciences*, *14*(24), 5789–5804. https://doi.org/10.5194/bg-14-5789-2017

Stal, L. J. (2009). Is the distribution of nitrogen-fixing cyanobacteria in the oceans related to temperature? *Environmental Microbiology*, *11*(7), 1632–1645. https://doi.org/10.1111/j.1758-2229.2009.00016.x

Stal, L. J., Albertano, P., Bergman, B., von Bröckel, K., Gallon, J. R., Hayes, P. K., et al. (2003). BASIC: Baltic Sea cyanobacteria. An investigation of the structure and dynamics of water blooms of cyanobacteria in the Baltic Sea—Responses to a changing environment. *Continental Shelf Research*, *23*(17–19), 1695–1714. https://doi.org/10.1016/j.csr.2003.06.001

Sternbeck, J., Sohlenius, G., & Hallberg, R. O. (2000). Sedimentary trace elements as proxies to depositional changes induced by a Holocene fresh-brackish water transition. *Aquatic Geochemistry*, *6*(3), 325–345. https://doi.org/10.1023/A:1009680714930

Szymczak-Żyła, M. (2018). CPPB-aE ($13^2,17^3$-cyclopheophorbide-a enol) in sediments—A potential proxy of oxygen deficiency in near-bottom water. *Organic Geochemistry*, *115*, 166–173. https://doi.org/10.1016/j.orggeochem.2017.10.011

Szymczak-Żyła, M., & Kowalewska, G. (2009). Chloropigments-a in sediments of the Gulf of Gdansk deposited during the last 4000 years as indicators of eutrophication and climate change. *Palaeogeography, Palaeoclimatology, Palaeocology*, *284*(3-4), 283–294. https://doi.org/10.1016/j.palaeo.2009.10.007

Szymczak-Żyła, M., Krajewska, M., Winogradow, A., Zaborska, A., Breedveld, G. D., & Kowalewska, G. (2017). Tracking trends in eutrophication based on pigments in recent coastal sediments. *Oceanologia*, *59*(1), 1–17. https://doi.org/10.1016/j.oceano.2016.08.003

Szymczak-Żyła, M., Louda, J. W., & Kowalewska, G. (2008). Comparison of extraction and HPLC methods for marine sedimentary chloropigment determinations. *Journal of Liquid Chromatography & Related Technologies*, *31*(8), 1162–1180. https://doi.org/10.1080/10826070802000699

Tonneijck, F. H., van der Plicht, J., Jansen, B., Verstraten, J. M., & Hooghiemstra, H. (2006). Radiocarbon dating of soil organic matter fractions in andosols in Northern Ecuador. *Radiocarbon*, *48*(03), 337–353. https://doi.org/10.1017/S0033822200038790

Tribovillard, N., Algeo, T. J., Lyons, T., & Riboulleau, A. (2006). Trace metals as paleoredox and paleoproductivity proxies: An update. *Chemical Geology*, *232*(1–2), 12–32. https://doi.org/10.1016/j.chemgeo.2006.02.012

Usero, J., Gamero, M., Morillo, J., & Gracia, I. (1998). Comparative study of three sequential extraction procedures for metals in marine sediments. *Environment International*, *24*(4), 487–496. https://doi.org/10.1016/S0160-4120(98)00028-2

Wasmund, N., Andrushaitis, A., Łysiak-Pastuszak, E., Müller-Karulis, B., Nausch, G., Neumann, T., et al. (2001). Trophic status of the southern-eastern Baltic Sea: A comparison of coastal and open areas. *Estuarine, Coastal and Shelf Science*, *53*(6), 849–864. https://doi.org/10.1006/ecss.2001.0828

Xue, B., Yao, S., & Xia, W. (2007). Environmental changes in Lake Taihu during the past century as recorded in sediment cores. *Hydrobiologia*, *581*(1), 117–123. https://doi.org/10.1007/s10750-006-0513-5

Zillén, L., Conley, D. J., Andrén, T., Andrén, E., & Björck, S. (2008). Past occurrences of hypoxia in the Baltic Sea and the role of climate variability, environmental change and human impact. *Earth-Science Reviews*, *91*(1–4), 77–92. https://doi.org/10.1016/j.earscirev.2008.10.001